DRAFT VERSION SEPTEMBER 29, 2014
Preprint typeset using LaTeX style emulateapj v. 08/13/06

arXiv:1407.0452v2 [astro-ph.SR] 26 Sep 2014

OPTICAL AND NEAR-INFRARED POLARIMETRY OF HIGHLY REDDENED TYPE IA SUPERNOVA 2014J: PECULIAR PROPERTIES OF DUST IN M82

K. S. KAWABATA[1,2], H. AKITAYA[1], M. YAMANAKA[3,4], R. ITOH[2,1], K. MAEDA[4,5], Y. MORITANI[1], T. UI[2], M. KAWABATA[2], K. MORI[2], D. NOGAMI[4], K. NOMOTO[5,13], N. SUZUKI[5], K. TAKAKI[2], M. TANAKA[6], I. UENO[2], S. CHIYONOBU[2], T. HARAO[2], R. MATSUI[2], H. MIYAMOTO[2], O. NAGAE[2], A. NAKASHIMA[7], H. NAKAYA[6], Y. OHASHI[2], T. OHSUGI[1], T. KOMATSU[2], K. SAKIMOTO[2], M. SASADA[4], H. SATO[2], H. TANAKA[2], T. URANO[2], T. YAMASHITA[6], M. YOSHIDA[1,2], A. ARAI[8], N. EBISUDA[2], Y. FUKAZAWA[2,1], A. FUKUI[9], O. HASHIMOTO[10], S. HONDA[8,10], H. IZUMIURA[9], Y. KANDA[2], K. KAWAGUCHI[2], N. KAWAI[11], D. KURODA[9], K. MASUMOTO[12], K. MATSUMOTO[12], T. NAKAOKA[2], K. TAKATA[2], M. UEMURA[1,2], AND K. YANAGISAWA[9]

Draft version September 29, 2014

ABSTRACT

We presented optical and near-infrared multi-band linear polarimetry of the highly reddened Type Ia SN 2014J appeared in M82. SN 2014J exhibits large polarization at shorter wavelengths, e.g., 4.8% in *B* band, and the polarization decreases rapidly at longer wavelengths, with the position angle of the polarization remaining at approximately 40° over the observed wavelength range. These polarimetric properties suggest that the observed polarization is likely to be caused predominantly by the interstellar dust within M82. Further analysis shows that the polarization peaks at a wavelengths much shorter than those obtained for the Galactic dust. The wavelength dependence of the polarization can be better described by an inverse power law rather than by Serkowski law for Galactic interstellar polarization. These suggests that the nature of the dust in M82 may be different from that in our Galaxy, with polarizing dust grains having a mean radius of < 0.1 μm .

Subject headings: dust, extinction — circumstellar matter — galaxies: individual (Messier 82) — supernovae: individual (SN 2014J) — polarization

1. INTRODUCTION

The homogeneity in photometric properties of normal Type Ia supernovae (SNe Ia) is expected to be related to common physical properties during the onset of thermonuclear explosions in the progenitor white dwarfs with a mass close to Chandrasekhar's limiting mass (Hillebrandt & Niemeyer 2000, for review). The continuum light from normal SNe Ia is intrinsically weakly polarized ($p \lesssim 0.3\%$), although the absorption features, including Si II 6355 and Ca II IR triplets, are often polarized by 0.5–1.5% (Wang et al. 1996; Wang, Wheeler, &Höflich 1997; Wang et al. 2003; Leonard et al. 2005; Wang et al. 2006; Wang and Wheeler 2008; Chornock & Filippenko 2008; Zelaya et al. 2013; Maund et al. 2013). In fact, a Si II 6355 absorption line with a polarization of $p = 1.5\%$ and an equivalent width of 0.011 μm (for SN 2014J near the maximum) gives an additional polarization of only $\Delta p = 0.13\%$ for typical R_C band polarimetry ($\Delta\lambda = 0.13$ μm). This practically allows us to use SNe Ia as a unique bright unpolarized-light source within distant galaxies for broadband polarimetry. Thus, a SN Ia has the potential to project the interstellar polarization (ISP) along the line of sight inside the host galaxy when subject to a substantial amount of interstellar reddening, as is commonly seen in our Galaxy (e.g., Whittet 2003).

SN 2014J is the closest SN Ia in this quarter century. It was discovered in M82 (at a distance $\sim 3.9 \pm 0.4$ Mpc; Sakai & Madore 1999) on 2014 Jan 21.81 (UT dates are used throughout this Letter) at a magnitude of $R = 10.99 \pm 0.03$ mag (Fossey et al. 2014; Goobar et al. 2014), probably a week after the explosion (Zheng et al. 2014). The apparent brightness provides us with an opportunity for various studies, including constraining early light curve model (Goobar et al. 2014; Zheng et al. 2014), studying progenitor systems (Kelly et al. 2014), and evaluating properties of extragalactic interstellar/circumstellar media (Amanullah et al. 2014; Foley et al. 2014; Welty et al. 2014). In addition, this SN provides a rare opportunity to probe the ISP within the starburst galaxy M82 because it suffers significant reddening from the host galaxy ($E^{\rm host}_{B-V} \sim 1.3$ mag). Prior to SN 2014J, there were only three reddened SNe Ia ($E^{\rm host}_{B-V} \geq 0.5$ mag) for which the wavelength dependence of optical polarization had been measured, which are SN 1986G in the peculiar giant S0 galaxy NGC 5128 (Cen A) (Hough et al. 1987; $E^{\rm host}_{B-V} \simeq 1.6$ mag and $d \simeq 4$ Mpc), SN 2006X in the Virgo Cluster spiral galaxy NGC 4321 (Patat et al. 2009; $E^{host}_{B-V} = 1.5$–1.7 mag and $d \simeq 16$ Mpc), and SN 2008fp in the peculiar spiral galaxy ESO 428-G14 (Cox & Patat 2014; $E^{host}_{B-V} = 0.6 \pm 0.1$ mag and $d \sim 26$ Mpc).

The Galactic ISP at ultraviolet (UV) to near-infrared (NIR) wavebands can be approximated by Serkowski law (Serkowski, Mathewson, & Ford 1975), a smooth function of

[1] Hiroshima Astrophysical Science Center, Hiroshima University, Kagamiyama, Higashi-Hiroshima, Hiroshima 739-8526, Japan; kawabtkj@hiroshima-u.ac.jp
[2] Department of Physical Science, Hiroshima University, Kagamiyama, Higashi-Hiroshima 739-8526, Japan
[3] Department of Physics, Faculty of Science and Engineering, Konan University, Okamoto, Kobe, Hyogo 658-8501, Japan
[4] Department of Astronomy, Graduate School of Science, Kyoto University, Sakyo-ku, Kyoto 606-8502, Japan
[5] Kavli Institute for the Physics and Mathematics of the Universe (WPI), The University of Tokyo, Kashiwa, Chiba 277-8583, Japan
[6] National Astronomical Observatory of Japan, Osawa, Mitaka, Tokyo 181-8588, Japan
[7] Nagoya City Science Museum, Sakae, Naka-ku, Nagoya 460-0008, Japan
[8] Nishi-Harima Astronomical Observatory, Center for Astronomy, University of Hyogo, Nishigaichi, Sayo-cho, Sayo, Hyogo 679-5313, Japan
[9] Okayama Astrophysical Observatory, NAOJ, Honjo, Kamogata-cho Asauchi, Okayama 719-0232, Japan
[10] Gunma Astronomical Observatory, Takayama, Gunma 377-0702
[11] Department of Physics, Tokyo Institute of Technology,Ookayama, Meguro-ku, Tokyo 152-8551, Japan
[12] Institute of Astronomy, Osaka Kyoiku University, Kashiwara, Osaka 582-8582, Japan
[13] Hamamatsu Professor

wavelength given by

$$p(\lambda) = p_{\max} \exp\left[-K \ln^2\left(\frac{\lambda_{\max}}{\lambda}\right)\right], \quad (1)$$

where $p_{\max}$ is the peak polarization degree occurring at wavelength $\lambda_{\max}$ and K is a parameter describing the width of the peak. The polarization observed for SNe 1986G and 2006X can be described by Serkowski law at optical wavelengths; however, the derived parameters are peculiar, i.e., the wavelengths $\lambda_{\max} = 0.43 \pm 0.01 \mu$m (SN 1986G) and $\lambda_{\max} = 0.35 \pm 0.01 \mu$m (SN 2006X) are significantly shorter than the Galactic value ($0.54 \pm 0.06 \mu$m; Vrba, Coyne, & Tapira 1981), and $K = 1.3 \pm 0.1$ (SN 2006X) is not consistent with the value expected from the Wilking law, i.e., $K = (1.66 \pm 0.09)\lambda_{\max}(\mu\text{m}) + (0.01 \pm 0.05)$, for the Galactic ISP (Wilking et al. 1980; Whittet et al. 1992). SN 2008fp exhibits interstellar polarization similar to the downscaled one of SN 2006X (Cox & Patat 2014). For the Galactic ISP, this $\lambda_{\max}$–K correlation may be interpreted as a narrowing in the size distribution with grain growth (e.g., Whittet 2003). The shorter $\lambda_{\max}$ with these SNe suggests that the size of the dust grains polarizing light in the host galaxies is, on average, smaller than those in the Milkyway. This is also consistent with the smaller values of the total-to-selective extinction ratio, i.e., $R_V = A_V/E_{B-V} \simeq 1.3$–$2.6$, obtained for some reddened SNe Ia (Phillips et al. 2013, and references therein). If the empirical relation of Galactic ISP, $R_V = (5.6 \pm 0.3)\lambda_{\max}(\mu\text{m})$ (Serkowski, Mathewson, & Ford 1975; Whittet 2003), still holds for small $\lambda_{\max}$, the observed values of $R_V \simeq 1.3$–2.6 corresponds to $\lambda_{\max} \simeq 0.23$–$0.46 \mu$m, which is comparable with $\lambda_{\max}$ observed in SNe 1986G and 2006X.

In this Letter, we report our $BVR_CI_CJHK_s$ polarimetry of SN 2014J before and after the maximum light, along with our photometric and spectroscopic observations. Such multi-band polarimetry including NIR bands for reddened SNe Ia is still quite rare, and therefore this SN may provide us a valuable information on the interstellar and/or circumstellar media along the line of sight toward SN 2014J within M82.

2. OBSERVATIONS AND REDUCTION

We performed imaging polarimetry of SN 2014J using Hiroshima One-shot Wide-field Polarimeter (HOWPol; Kawabata et al. 2008) on 2014 Jan 22.4 ($t = -11.0$ days relative to the B-band maximum light; see §3.1) in VR_CI_C bands and Hiroshima Optical and Near IR camera (HONIR; Akitaya et al. 2014) in $BVR_CI_CJHK_s$ bands on Jan 27.7 (–5.7 days), Feb 16.5 (+14.1 days), 25.6 (+23.2 days) and Mar 7.8 (+33.4 days). HOWPol employs a wedged double Wollaston prism, and is attached to the Nasmyth focus of the 1.5 m Kanata telescope at Higashi-Hiroshima Observatory. HONIR uses a cooled $LiYF_4$ Wollaston prism and is attached to the Cassegrain focus of the same telescope. Each observation consisted of a sequence of exposures at four position angles (PAs) of the achromatic half-wave plates, 0.°0, 22.°5, 45.°0, and 67.°5 for the HOWPol and the last HONIR observations, and at four PAs of the instrumental rotator at the Cassegrain focus of the telescope, 0°, 90°, 45° and 135°, for the first three HONIR observations. These data were calibrated using observations of unpolarized (HD 94851, HD 98281) and polarized standard stars (HD 30168, HD 150193, HDE 283701, Cyg OB 2 #11; Turnshek et al. 1990; Whittet et al. 1992), including measurements through a fully-polarizing filter or a wire grid. Using this procedure, the instrumental polarization ($p \lesssim 0.2\%$ in HONIR and $p \simeq 3$–4% in HOWPol) was vectorially removed.

In addition, we obtained photometry using HOWPol (BVR_CI_C), and HONIR ($BVR_CI_CJHK_s$) attached to the 1.5-m Kanata telescope, with MITSuME (Kotani et al. 2005) ($g'R_CI_C$) attached to the 0.5 m telescope at Okayama Astrophysical Observatory (OAO) of National Astronomical Observatory of Japan, with a Peltier-cooled CCD (BVR_CI_C) attached to the 0.51 m telescope at Osaka Kyoiku University (OKU), and with ISLE (Yanagisawa et al. 2008) (JHK_s) attached to the 1.88 m telescope at OAO, respectively. The magnitude in each band was determined relative to the nearby comparison star, BD+70°587, which was flux-calibrated in BVR_CI_C bands using Landolt field stars (Landolt 1992) on a photometric night. For NIR photometry, we used JHK_s magnitudes of the same star in 2MASS Second Incremental Release Point Source Catalogue. We also collected low-resolution spectra with HOWPol (0.41–0.94 μm, $R = \lambda/\Delta\lambda \simeq 400$) and HONIR (0.5–2.3 μm, $R \simeq 450$–600) on the 1.5-m Kanata telescope. The flux was calibrated using observations of spectrophotometric standard stars obtained on the same nights.

Because SN 2014J is superimposed within the bright region of M82 and we cannot perform template subtraction in image reduction, the obtained flux should be more or less contaminated by the inhomogeneity and irregularity of the surface brightness of M82. However, the SN itself is sufficiently bright, and the polarizations obtained during the period from $t = -11$ days to $t = +33$ days from the maximum light should suffer minor effects from the galaxy light.

3. RESULTS

3.1. *Photometric and Spectroscopic Properties*

Figure 1 shows the obtained multi-band light curves (LCs). The apparent maximum magnitudes in BV bands are found to be $B_{\max} = 11.99 \pm 0.05$ mag on MJD 56690.4 ± 0.5 (Feb 2.4 ± 0.5) and $V_{\max} = 10.44 \pm 0.03$ mag on MJD 56691.7 ± 0.5, respectively, as derived by a polynomial fit to the observed data around the maximum light. We also derived the observed B-band magnitude decline rate $\Delta m_{15}(B) = 1.02 \pm 0.05$ mag. For the extinction toward SN 2014J, Amanullah et al. (2014) estimated the total reddening of $E_{B-V}^{\text{total}} = 1.37 \pm 0.03$ mag and $R_V^{\text{total}} = 1.4 \pm 0.1$ based on analysis of near-maximum-light spectral energy distribution from UV to NIR wavebands. This reddening is apparently dominated by the host galaxy component E_{B-V}^{host}, because the IR Dustmap suggests that the Galactic component is only $E_{B-V}^{\text{MW}} = 0.14$ mag (Schlafly & Finkbeiner 2011). We corrected for the extinction using the E_{B-V}^{total} and R_V^{total} values and the parameterized extinction curve (Cardelli, Clayton, & Mathis 1989). The absolute magnitudes of $M_{B,\max} = -19.26 \pm 0.26$ mag and $M_{V,\max} = -19.42 \pm 0.25$ mag, as well as its color, are consistent with the empirical relations with $\Delta m_B(15)$ within errors (e.g., Phillips et al. 1999), suggesting the photometric behavior in SN 2014J is not anomalous. We set the time of the B band maximum as $t = 0$ days, which is 18.7 ± 0.5 days after the epoch of the estimated first light (Zheng et al. 2014; Goobar et al. 2014).

Figure 2 shows a time series of spectra from $t = -11$ days to $t = +48$ days. Compared with the normal SN Ia 2011fe, SN 2014J is characterized by the absence of spectral features due to C II 6580 and O I 7774, as well as the existence of high-velocity components in Ca II IR triplet ($\gtrsim 20,000$ km s^{-1}) during the earliest phase $t \lesssim -5$ days, as pointed out by Goobar

et al. (2014). The line velocity and equivalent width of Si II 6355 around maximum ($-2 < t < 2$ days) are $-11,750 \pm 300$ km s^{-1} (Figure 2 inset panel) and 110 ± 5 Å, respectively, which are marginal between those of 'Normal' and 'HV' SNe (Wang et al. 2009). However, the relation between Δm_{15}-corrected $M_{V,\max}$ and $E^{\rm host}_{B-V}$ yielded in SN 2014J (~ -17.9 mag for $M_{V,\max}$ and ~ 1.23 mag for $E^{\rm host}_{B-V}$) is apparently consistent with the branch of HV group ($R_V \sim 1.6$; Wang et al. 2009). The nearly constant absorption strength (up to ~ 3 months after discovery) of the interstellar Na I D lines and diffuse interstellar bands (e.g., Welty et al. 2014) indicate that the dust responsible for the extinction towards SN 2014J is located at a site moderately separated from the progenitor ($\gtrsim 2 \times 10^{16}$ cm).

3.2. *Polarimetric Properties*

The observed polarization is shown in Figure 3. The polarization is relatively strong in blue bands, e.g., reaching $\sim 4.8\%$ in B band, and it decreases rapidly with wavelength, while the polarization PA is approximately constant at around 40°. In NIR bands, the polarization is less significant ($p \lesssim 1\%$); however, it is likely that the same polarization component still dominates because of having almost the same PA as the optical bands. There is no significant temporal variation in the polarization measured during the period from $t = -11$ days to $t = +33$ days from the maximum light, and the polarization in optical bands appears to be consistent with the result of spectropolarimetry covering wavelengths from 380 to 880 nm (Patat et al. 2014). Hereafter, we discuss only the averaged polarization (Table 1).

The large polarization measured for SN 2014J suggests that it is predominantly produced within M82, because the Galactic ISP is, at most, 0.18% according to the measurements of six Galactic stars in the vicinity of SN 2014J within 10° of the all-sky polarization map (Heiles 2000). Furthermore, the almost constant polarization during the period of our observation would exclude the possibility that it is originated in the close proximity to the progenitor. This, together with the unchanged interstellar absorption lines, favors that that the significant polarization of SN 2014J is caused by dust grains at a site remote from the SN. It has been suggested that multiple scattering due to circumstellar (CS) dust may account for half of the total extinction (Foley et al. 2014). However, we argue that the CS dust could not be the principal origin of the observed polarization because multiple scattering would effectively depolarize the light and the resulting continuum polarization would also show significant changes with time (see also Patat et al. 2014). In the optical image of M82 (e.g., Ohyama et al. 2002), PA of $\sim 40°$ seems to align with the direction of the local dust lanes around the SN position, which further strengthens the argument that the polarization is unrelated to the CS matter.

Figure 3 shows that the polarization peak appears outside the wavelength range of our observations, i.e., $\lambda_{\max} \lesssim 0.4 \mu$m. This $\lambda_{\max}$ is considerably smaller than the typical value determined from the Galactic ISP. For comparison, we also plotted the polarization curves determined from the Serkowski law with/without the Wilking law in Figure 3. For the Serkowski law, we fitted it with a constant $K \equiv 1.15$, a typical one for Galactic ISP (Serkowski, Mathewson, & Ford 1975), because the fitted parameters do not converge in case of free K. We cannot obtain any good fit with the Wilking law. In general, with the Wilking law, a short $\lambda_{\max}$ leads to small K (corresponding to broader peak in $p(\lambda)$ curve); however, the observed steep gradient of $p(\lambda)$ requires a large K value. The Wilking law also fails to describe the continuum polarization measured for SN 2006X (Patat et al. 2009). In addition, we find that $K = 1.13 \pm 0.05$ and $\lambda_{\max} = 0.43 \pm 0.01 \mu$m derived for the SN 1986G data (Hough et al. 1987) do not satisfy the Wilking law. The fact that 5 out of 105 Galactic reddened stars show considerable ISP with $\lambda_{\max} < 0.4 \mu$m and the Wilking law holds for 4 of the 5 stars within the errors (Whittet et al. 1992) suggests that the failure of the Wilking law to describe the data may be common for highly reddened SNe Ia and the dust properties of the host galaxies may differ from those of the Milkyway.

Using only Serkowski law, we note that there is a systematic difference in the polarization of $\Delta p = 0.2$–0.3% between the observed polarization and the fitted curve at longer wavelengths ($\gtrsim 1 \mu$m, Figure 3). This difference may be explained by considering an analog of the 'IR polarization excess' found in the Galactic ISP at longer wavelengths ($\gtrsim 2 \mu$m), which is characterized by an inverse power-law, i.e., $p(\lambda)$ (e.g., Nagata 1990). The wavelength dependence of polarization of SN 2014J at $\gtrsim 0.5 \mu$m can be well described by $p(\lambda) = p_1 \lambda^{-\beta}$ with the index of $\beta = 2.23 \pm 0.10$ (Figure 4). It should be noted that the polarization closely follows a power-law dependence even at the optical wavelengths for SN 2014J. For Galactic reddened stars, the index β is typically in a relatively narrow range of 1.5–2.0 and is uncorrelated with the wavelength dependence of optical polarization, e.g., $\lambda_{\max}$ (Martin et al. 1992; Whittet 2003). The index β obtained for the ISP in M82 appears slightly steeper than that for the Galactic ISP. This may be related to the failure of the Wilking law, because the polarization peak observed in SN 2014J is clearly sharper than that expected for a Galactic ISP with a similar $\lambda_{\max}$ (see Figure 3).

4. DISCUSSION

As described above, SN 2014J is a highly reddened SN Ia, similar to SNe 1986G, 2006X and 2008fp. The blue continuum of these SNe Ia all exhibit significant polarization, which is atypical of a Galactic ISP. To a first-order approximation, a small $\lambda_{\max}$ corresponds to small mean size of the dust grains causing the observed polarization. This can be explained using Mie theory for dielectric cylinders, e.g., $\lambda_{\max} \sim 2\pi a_{\rm eff}(n-1)$, where $a_{\rm eff}$ is the effective radius and n is refractive index of the cylindrical grain (e.g., Whittet 2003). Assuming $\lambda_{\max} \lesssim 0.4 \mu$m and $n = 1.6$ (appropriate for silicates), then $a_{\rm eff}$ of the polarizing grains should be $\lesssim 0.11 \mu$m. Although a small $\lambda_{\max}$ (and thus a small $a_{\rm eff}$) could be the result of a failure of alignment/asphericity only of larger grains, the small R_V inferred for SN 2014J suggests that the effect is not significant and the grain size should be intrinsically small.

It is not known whether the empirical relation $R_V = (5.6 \pm 0.3)\lambda_{\max}(\mu{\rm m})$ determined for the Galactic ISP (Serkowski, Mathewson, & Ford 1975; Whittet 2003) holds in the host galaxies of these highly reddened SNe Ia; however, interestingly, it has been shown that R_V is small for these SNe, e.g., $2.57^{+0.23}_{-0.21}$ for SN 1986G and $1.31^{+0.08}_{-0.10}$ for SN 2006X (Table 2 in Phillips et al. 2013) and the $\lambda_{\max} = 0.43 \pm 0.01 \mu$m obtained for SN 1986G (Hough et al. 1987) satisfies the empirical relation within the errors. For SN 2006X, $R_V = 1.31$ is much smaller than that expected from $\lambda_{\max} \sim 0.35 \mu$m (i.e., $R_V = 2.0 \pm 0.1$). Wang et al. (2008) derived a slightly larger value of $R_V \sim 1.5$ from optical and NIR photometry of SN 2006X; however, this is still smaller than the expected value.

TABLE 1
MEASURED POLARIZATION OF SN 2014J

Band	p (%)[a]	PA[a]	Band	p (%)[a]	PA[a]
B	4.79±0.58	$43.^\circ2 \pm 1.^\circ8$	J	0.63±0.06	$44.^\circ8 \pm 3.^\circ3$
V	3.69±0.14	$37.^\circ3 \pm 1.^\circ1$	H	0.35±0.06	$39.^\circ5 \pm 2.^\circ5$
R_C	2.36±0.06	$38.^\circ8 \pm 0.^\circ9$	K_s	0.12±0.10	$43.^\circ8 \pm 14.^\circ6$
I_C	1.42±0.08	$39.^\circ8 \pm 1.^\circ4$			

[a] Averaged polarization and the position angle are shown (see §3.2). In VRI bands the data are weighted means over five nights from t = −11 days through t = +33 days, and in other bands they are over four nights from t = −6 days through +33 days. The error is predominantly due either to the observational error (σ) in $R_C I_C JHK_s$ bands or the uncertainty of the polarimetric calibration (instrumental polarization/depolarization) in BV bands.

It should be noted that $\lambda_{\rm max}$ is somewhat ambiguous because the observations did not cover the wavelengths shorter than 0.35 μm (Patat et al. 2009), which makes it difficult to completely rule out the applicability of the empirical relation. For SN 2014J, $R_V^{\rm total} = 1.4 \pm 0.1$ (Amanullah et al. 2014), which leads to $\lambda_{\rm max} = 0.25 \pm 0.02$ μm, which is speculatively consistent with the result of our fit to Serkowski law with a constant K = 1.15. Therefore, although the Wilking law (i.e., $\lambda_{\rm max}$–K relation) no longer appears to be valid for extragalactic ISPs (see §3.2), the positive correlation of $\lambda_{\rm max}$–R_V may hold even for an ISP with $\lambda_{\rm max} < 0.4$ μm, at least, in part of the extragalactic environment. If this is indeed the case, the smaller values of R_V seen in some moderately to highly reddened SNe Ia (e.g., Phillips et al. 2013) suggests that the ISP in the host galaxies has a smaller $\lambda_{\rm max}$, and hence a smaller $a_{\rm eff}$. The failure of the data to follow the Wilking law is harder to be explain using grain sizes only; a qualitative difference in the size distribution (and possibly in composition, shape, and degree of alignment) would be required for the dust grains between our Galaxy and those host galaxies of SNe Ia. A possible explanation for the atypical dust seen in the host galaxies of some SNe Ia is that the interstellar dust within our Galaxy is not in fact typical. The understanding of physical properties of extragalactic dust grains remains incomplete. Extensive data on the UV and optical polarimetry for SNe Ia may therefore be crucial for further understanding of the properties of extragalactic dust.

This work was supported by JSPS Research Fellowships for Young Scientists (KT), by the Grant-in-Aid for Scientific Research from JSPS (23340048,23740141,26287031,26800100), and by Optical and NIR Astronomy Inter-University Cooperation Program, OISTER, and by WPI Initiative, from the Ministry of Education, Culture, Sports, Science, and Technology in Japan.

REFERENCES

Akitaya, H., Moritani, Y., Ui, T., et al. 2014, Proc. SPIE, 9147, 91474O
Amanullah, R., Goobar, A., Johansson, J., et al. 2014, ApJ, 788, L21
Cardelli, J. A., Clayton, G. C., & Mathis, J. S. 1989, ApJ, 345, 245
Chornock, R., & Filippenko, A. V. 2008, AJ, 136, 2227
Cox, N. L. J., & Patat, F. 2014, A&A, 565, A61
Fossey, S., Cooke, B., Pollack, G., Wilde, M., & Wright, T. 2014, CBET, 3792, 1
Foley, R. J., Fox, O., McCully, C., Phillips, M. M., Sand, D. J., et al. 2014, MNRAS, submitted (arXiv: 1405.3677)
Goobar, A., Johansson, J., Amanullah, R., et al. 2014, ApJ, 784, L12
Heiles, C. 2000, AJ, 119, 923
Hillebrandt, W., & Niemeyer, J. C. 2000, ARA&A, 38, 191
Hough, J. H., Bailey, J. A., Rouse, M. F., & Whittet, D. C. B. 1987,MNRAS, 227, 1
Hutton, S., Ferreras, I., Wu, K., et al. 2014, MNRAS, 440, 150
Kawabata, K. S., Nagae, O., Chiyonobu, S., et al. 2008, Proc. SPIE, 7014, 70144L
Kelly, P. L., Fox, O. D., Filippenko, A. V., et al. 2014, ApJ, 790, 3
Kotani, T., Kawai, N., Yanagisawa, K., et al. 2005, NCimC, 28, 755
Leonard, D. C., Li, W., Filippenko, A. V., Foley, R. J., & Chornock, R. 2005, ApJ, 632, 450
Landolt, A. U. 1992, AJ, 104, 340
Marion, G. H., Sand, D. J., Hsiao, E. Y., Banerjee, D. P. K., Valenti, S., et al., ApJ, submitted (arXiv: 1405.3970)
Martin, P. G., Adamson, A. J., Whittet, D. C. B., et al. 1992, ApJ, 392, 691
Matheson, T, Joyce, R. R., Allen, L. E. et al. 2012, ApJ, 754, 19
Maund, J. R., Spyromilio, J., Höflich, P. A., et al. 2013 MNRAS, 433, L20
Nagata, T. 1990, ApJ, 348, L13
Ohyama, Y., Taniguchi, Y., Iye, M., et al. 2002, PASJ, 54, 891
Patat, F., Baade, D., Höflich, P, et al. 2009, A&A, 508, 229
Patat, F., Taubenberger, S., Cox, N. L. J., et al. 2014, A&A, submitted (arXiv: 1407.0136)
Pereira, R., Thomas, R. C., Aldering, G., et al. 2013, A&A, 554, A27
Phillips, M. M., Lira, P., Suntzeff, N. B., et al. 1999, AJ, 118, 1766
Phillips, M. M., Simon J. D., Morrell, N., et al. 2013, ApJ, 779, 38
Richmond, M. W., & Smith, H. A. 2012, JAVSO, 40, 872
Sakai, S., & Madore, B. F. 1999, ApJ, 526, 599
Schlafly, E. F., & Finkbeiner, D. P. 2011, ApJ, 737, 103
Serkowski, K., Mathewson, D. S., & Ford, V. L. 1975, ApJ, 196, 261
Shappee, B. J. & Stanek, K. Z. 2011, ApJ, 733, 124
Smith, P. S., Williams, G. G., Smith, N., Milne, P. A., Jannuzi, B. T., & Green, E. M. 2014, ApJ, submitted (arXiv: 1111, 6626)
Turnshek, D. A., Bohlin, R. C., Williamson, R. L., II, et al. 1990, AJ, 99, 1243
Vrba, F. J., Coyne, G. V., & Tapia, S. 1981, ApJ, 243, 489
Wang, L., Wheeler, J. C., Li, Z., & Clocchiatti, A. 1996, ApJ, 467, 435
Wang, L., Wheeler, J. C., & Höflich, P. 1997, ApJ, 476, 27
Wang, L., Baade, D., Höflich, P., et al. 2003, ApJ, 591, 1110
Wang, L., Baade, D., Höflich, P., et al. 2006, ApJ, 653, 490
Wang, L., & Wheeler, J. C. 2008, ARA&A, 46, 433
Wang, X., Li, W., Filippenko, A. V., et al. 2008, ApJ, 675, 626
Wang, X., Filippenko, A. V., Ganeshalingam, M., et al. 2009, ApJ, 699, L139
Welty, D. E., Ritchey, A. M., Dahlstrom, J. A., & York, D. G. 2014, arXiv: 1404.2639
Whittet, D. C. B., Martin, P. G., Hough, J. H., et al. 1992, ApJ, 386, 562
Whittet, D. C. B. 2003, Dust in the Galactic Environment (2nd ed.; Bristol; IOP)
Wilking, B. A., Lebofsky, M. J., Kemp, J. C., Martin, P. G., & Rieke, G. H. 1980, ApJ, 235, 905
Yanagisawa, K., Okita, K., Shimizu, Y., et al. 2008, Proc. SPIE, 7014, 701437
Zelaya, P., Quinn, J. R., Baae, D., et al. 2013, AJ, 145, 27
Zheng, W., Shivvers, I., Filippenko, A. V., et al. 2014, ApJ, 783, L24

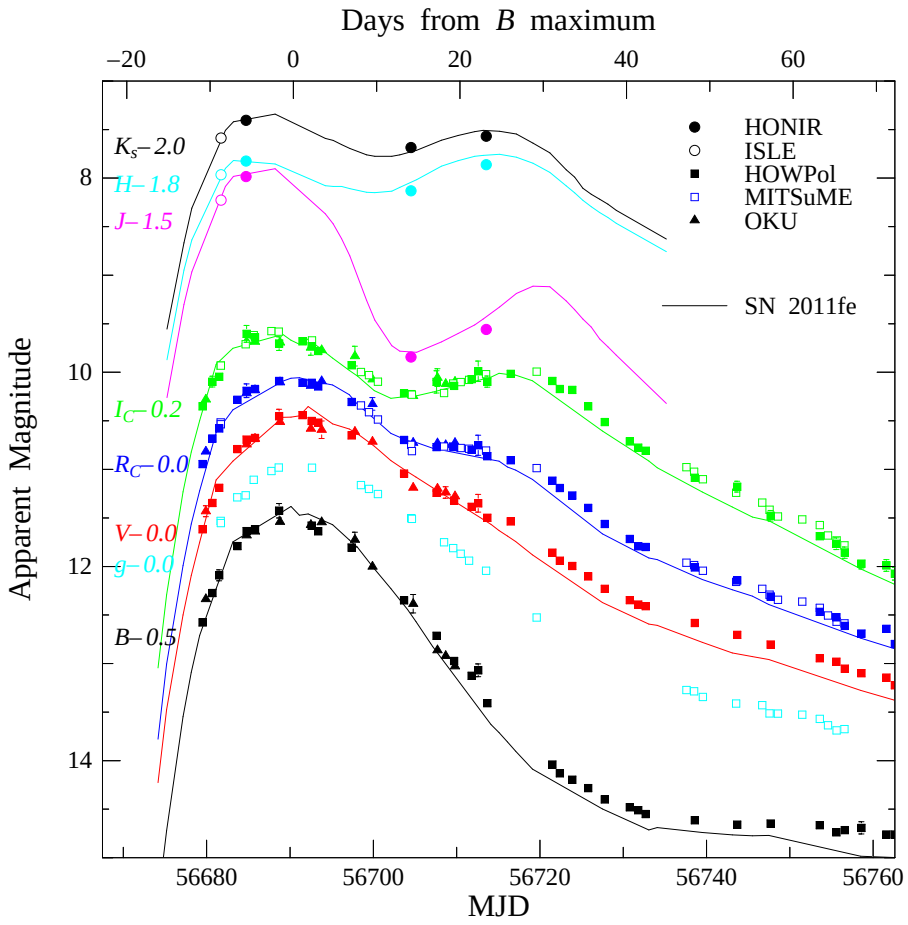

FIG. 1.— Multi-band light curves (LCs) of SN 2014J. We also plot LCs of normal SN Ia 2011fe ($\Delta m_B(15) = 1.21 \pm 0.03$ mag; Richmond & Smith 2012; Matheson et al. 2012) for comparison, which are shifted to match the peak time and magnitudes.

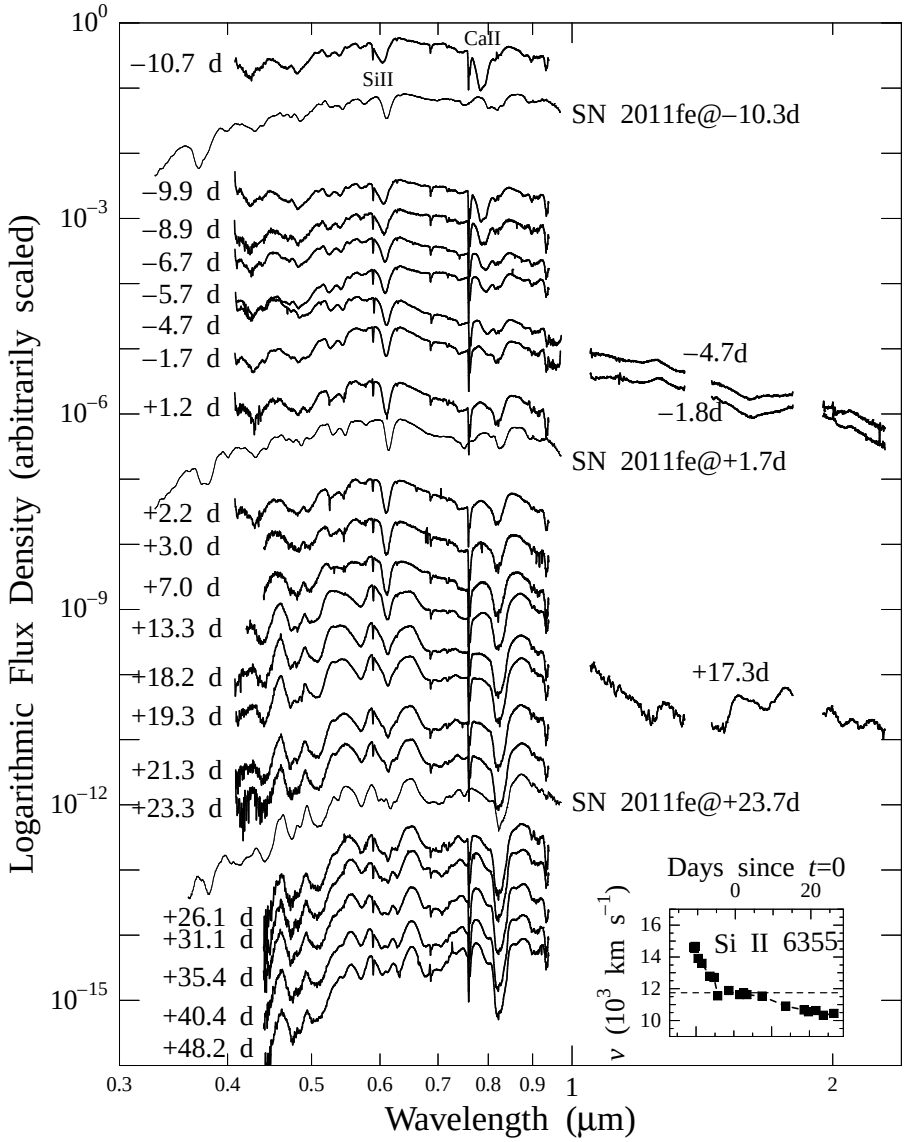

FIG. 2.— Spectral evolution of SN 2014J. The epoch of each spectrum is indicated in the panel. For comparison, we also plot optical spectra of SN 2011fe at three epochs (Pereira et al. 2013), reddened with E_{B-V} = 1.37 and R_V = 1.4 to match those of SN 2014J. The inset panel shows the evolution of the line velocity of Si II 6355 and the horizontal dashed line shows the velocity at around t = 0 days (see 3.1).

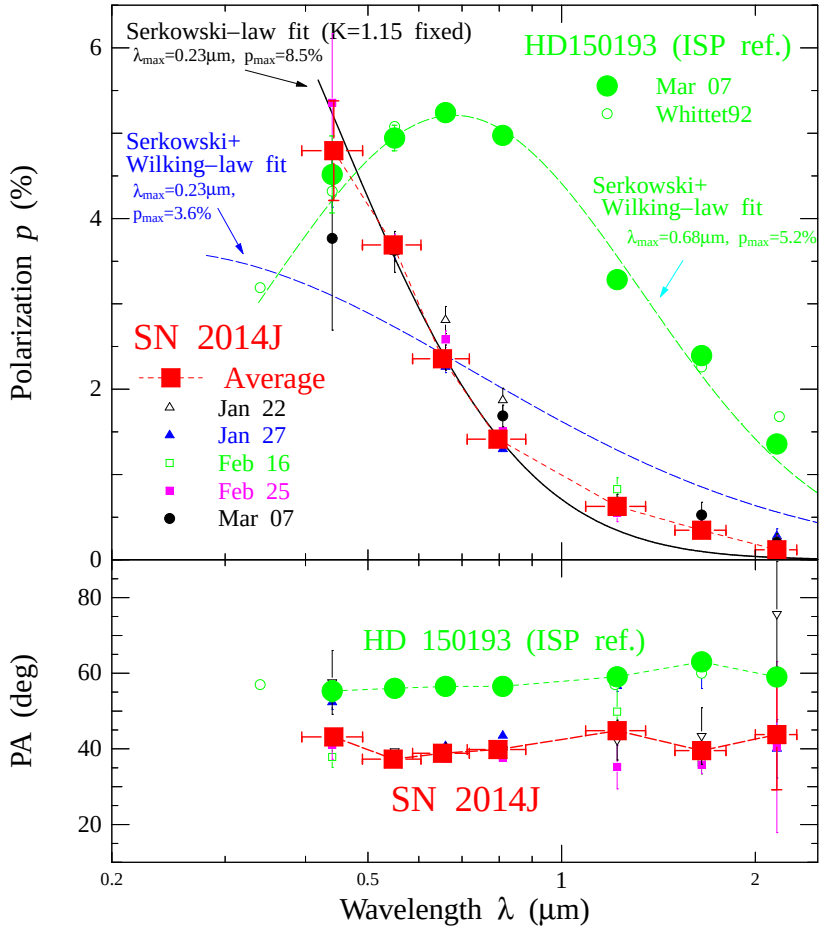

FIG. 3.— Result of our multi-band polarimetry. The upper panel shows the degree of polarization and the lower panel shows the position angle on the projected sky. The red squares denote the polarization of SN 2014J averaged over all five/four nights (Table 1), and the small symbols show the individual nightly data, as indicated. The curves in the panel show the empirical laws of the Galactic ISP, Serkowski law (black line), and that with Wilking law (blue dashed line), fitted to the averaged polarization data at optical wavelengths ($\lambda < 1$ μm). For comparison, we plot the observed/cataloged polarization (green circles/dots) of the strongly-polarized standard star, HD 150193 (Whittet et al. 1992), as a typical $p(\lambda)$ curve of Galactic ISP. It is clear that the strong wavelength dependence of SN 2014J is not readily explained by the Wilking law.

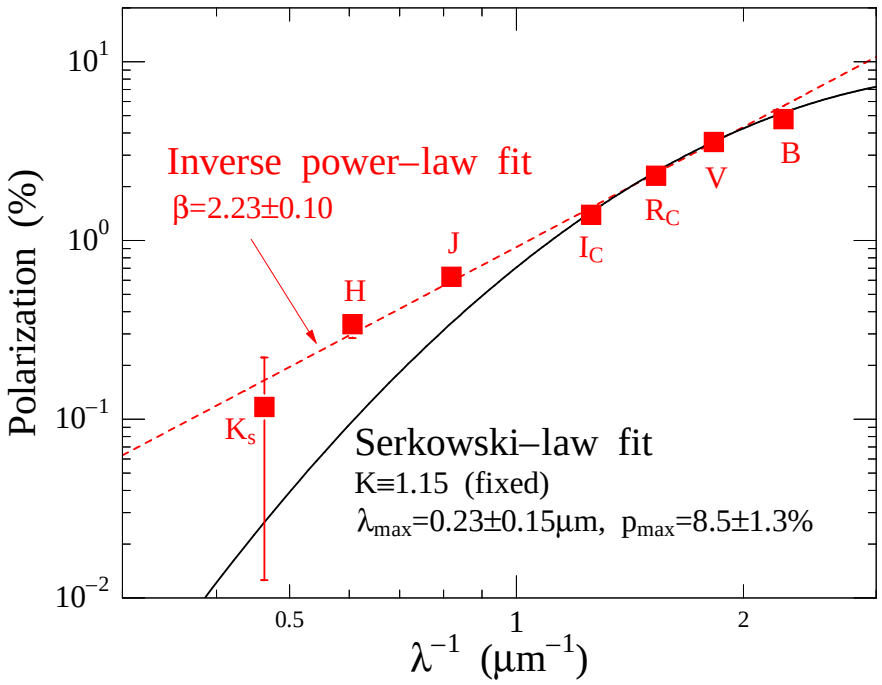

FIG. 4.— Polarization curve of SN 2014J as a function of the inverse wavelength plotted on logarithmic axes. The red squares and the black line are the same in Fig. 3. The red dashed straight line shows a power-law fit to the polarization data reported in this paper, except for *B*-band data. The wavelength dependence of polarization at regions with $\lambda > 0.5$ μm can be better explained by $\propto \lambda^{-(2.23\pm0.10)}$, rather than Serkowski law (black line).